

Acrolein induces axolemmal disruption, oxidative stress, and mitochondrial impairment in spinal cord tissue

Jian Luo, Riyi Shi*

*Department of Basic Medical Sciences, Center for Paralysis Research, Institute for Applied Neurology,
School of Veterinary Medicine, Purdue University, West Lafayette, IN 47907, USA*

Received 3 June 2003; received in revised form 28 August 2003; accepted 15 September 2003

Abstract

Acrolein, a byproduct of oxidative stress and lipid peroxidation, has been implicated in neurodegenerative disorders such as Alzheimer's disease, but not in spinal cord trauma, as a possible key factor in neuronal degeneration. Using an isolated guinea pig spinal cord model, we have found that acrolein, in a dose- and time-dependent manner, inflicts severe membrane disruption, a factor thought to be critical in triggering axonal deterioration and cell death. The concentration threshold of such detrimental effect is shown to be around 1 μ M when acrolein was exposed for 4 h. The membrane damage is likely mediated in part by reactive oxygen species and lipid peroxidation, which were elevated in response to acrolein exposure. Antioxidants were able to significantly reduce acrolein-mediated membrane disruption which further supports the role of reactive oxygen species in the loss of membrane integrity. Mitochondrial function was also impaired after acrolein exposure which not only implicates but emphasizes the role of this organelle in reactive oxygen species generation.

In summary, our data strongly suggest that at a clinically relevant concentration, acrolein can severely compromise membrane integrity and may further serve as an initiating toxin triggering secondary injury cascades following the initial physical insult to the spinal cord.

© 2003 Elsevier Ltd. All rights reserved.

Keywords: Membrane damage; Lipid peroxidation; Reactive oxygen species; Antioxidants; Guinea pig; Synaptosome

1. Introduction

Lipid peroxidation (LPO), resulting from reactive oxygen species (ROS)-induced damage to polyunsaturated fatty acids in the plasma membranes, occurs in traumatic central nervous system injuries (Hall, 1996; Lewen et al., 2000; Povlishock and Kontos, 1992) and in neurodegenerative disorders such as Alzheimer's and Parkinson's diseases (Coyle and Puttfarcken, 1993; Farooqui and Horrocks, 1998). Lipid peroxidation generates cytotoxic aldehydic byproducts such as 4-hydroxynonenal (HNE) and 2-propenal, also known as acrolein (Esterbauer et al., 1991; Uchida, 1999; Uchida et al., 1998). It has been shown that HNE accumulates rapidly after spinal cord injury (SCI) (Baldwin et al., 1998; Springer et al., 1997) and that acrolein is present in significant amounts in the brain of patients with Alzheimer's disease (Lovell et al., 2001). Since these alkenals are known to be potent neurotoxins (Kehrer and Biswal, 2000) and their lifetime is much longer than the short-lived ROS (Esterbauer et al., 1991), their accumulation is likely essential to the pathogenesis of SCI and neurodegenerative

diseases. Available data indicates that, compared to other alkenals such as HNE, acrolein may play a particularly important role in inflicting damage to cells, since it is the most reactive and thus toxic of all known alkenals (Dennis and Shibamoto, 1990; Esterbauer et al., 1991; Lovell et al., 2000).

In spite of extensive studies of acrolein toxicity, there is still an incomplete understanding of the magnitude of its effect and the mechanisms of its action. In particular, the detrimental effect of acrolein on neuronal plasma membrane has not been examined in detail. Since lipid peroxidation occurs within the membrane, the plasma membrane is the first, and perhaps most important, target of acrolein. Furthermore, there is strong evidence from experimental spinal cord injury studies that membrane damage is the pivotal event in initiating the primary and secondary events mediating axonal injury, which leads to cell death, tissue loss, and permanent neurological dysfunction (Krause et al., 1994; Meiri et al., 1981; Pettus et al., 1994; Shi et al., 2000; Xie and Barrett, 1991; Yawo and Kuno, 1983). Therefore, it is logical to hypothesize that acrolein plays a critical role in secondary injury following spinal cord and brain trauma. Our long-term goal is to examine the mechanism of secondary injury and, in particular, the linkage of these

* Corresponding author. Tel.: +1-765-496-3018; fax: +1-765-494-7605.
E-mail address: riyi@purdue.edu (R. Shi).

two critical factors in traumatic spinal cord injury: acrolein accumulation and membrane disruption.

In this study, we intend to examine the dose and time dependence of acrolein-mediated membrane disruption. This investigation was carried out in an isolated guinea pig spinal cord model, aiming to exclude the uncontrolled variables typical of *in vivo* studies. To characterize the dynamics and the magnitude of membrane disruption, we used three molecular markers of different sizes to estimate the size of breaches in the membrane after acrolein-induced membrane disruption.

Previous investigations suggest that acrolein, a byproduct of free radical-mediated lipid peroxidation itself, may exert its detrimental effect through ROS generation and lipid peroxidation (Adams Jr. and Klaidman, 1993; Patel, 1987). It is possible that acrolein may exert its membrane damaging effects through the generation of ROS and LPO, which could continuously and progressively worsen axolemmal disruption through self-reinforcing positive feedback. Furthermore, since mitochondria are organelles critical for cellular function as well as a rich source of ROS (Droge, 2002; Lenaz, 2001), they may also be involved in the cycle of acrolein-mediated membrane damage. Despite the potentially important roles mitochondria may play in acrolein toxicity, these possible mechanisms have not been tested in a spinal cord tissue model. By unveiling the characteristics and mechanisms of acrolein-mediated membrane damage, the result of this study not only broadens our understanding of acrolein toxicity in spinal cord trauma, but also suggests possible therapeutic interventions.

2. Experimental procedures

2.1. Preparation of spinal cord strips

All animals used in this study were handled in strict accordance with the NIH Guide for the Care and Use of Laboratory Animals and the experimental protocol was approved by the Purdue Animal Care and Usage Committee. In these experiments, every effort was made to reduce the number and suffering of the animals used. Spinal cord strips were prepared as previously described (Luo et al., 2002; Shi et al., 2002). Briefly, adult female Hartley guinea pigs were anesthetized deeply with ketamine (60 mg/kg) and xylazine (10 mg/kg), and were then perfused through the heart with 500 ml of oxygenated, cold Krebs' solution. The spinal cord was removed from the vertebrae and separated into two halves by midline sagittal division. The cord was then cut into segments weighing about 100 mg (3 cm long). These segments were maintained in oxygenated Krebs' solution at 37°C for 1 h before the onset of the experiment.

One hour after isolation, each spinal cord strip was exposed to 1, 10, 25, 50, 100 or 200 μ M acrolein in a volume

of 15 ml for 4 h. In the experiments examining the time dependence of acrolein toxicity, the cord was exposed to a fixed level of acrolein for 15 min, 1, 2, or 4 h. The acrolein stock solution was made every day using the Krebs' solution. The strips were immersed in the acrolein solutions which were oxygenated during the experiment time and protected from light.

2.2. Application of antioxidants

Cell-permeable ROS scavengers sodium formate (15 mM, hydroxyl radical scavenger), PEG-catalase (500 U/ml, hydrogen peroxide scavenger), Mn(III)tetrakis(*N*-methyl-4'-pyridyl) porphyrin (MnTMPyP, 25 μ M, superoxide scavenger), glutathione ethyl ester (GEE, 2 mM) were made fresh immediately before use. The antioxidants were added into the incubating medium immediately after the spinal cord was exposed to 200 μ M acrolein. Pretreatment with GEE was carried out by immersing the spinal cord strips in the Krebs' solutions containing 2 mM GEE for 2 h before acrolein application.

2.3. Measurement of plasma membrane damage

The plasma membrane damage induced by acrolein exposure was determined using three molecules with different molecular weights: ethidium bromide (EB, MW = 400 Da), horseradish peroxidase (HRP, MW = 44 kDa, type VI) and lactate dehydrogenase (LDH, MW = 140 kDa) (Luo et al., 2002; Shi and Borgens, 2000; Shi and Pryor, 2000; Shi et al., 2000). Ethidium bromide and HRP were added to the solution and the uptake of EB and HRP through the membrane breach of the exposed cord strips was quantified. Specifically, EB fluorescence intensity and the numbers of HRP-labeled axons were determined. These intracellular markers were thus used as an indicator of the size and the extent of membrane damage (Luo et al., 2002). The fluorescence intensity of EB in the spinal cord tissue was quantified using Sigmascan Pro (SPSS Science, Chicago, IL). To compensate for the variation of the fluorescent intensity of each individual image, all ethidium bromide fluorescence values of cord tissues were corrected for background fluorescence and expressed as a percentage relative to control (Luo et al., 2002). Briefly, four smaller areas (5% of the total field) were randomly selected at each corner (outside of the spinal cord tissue) and the average fluorescence intensity of these four areas was used as background intensity. The fluorescence intensity of the spinal cord samples was obtained by subtracting the background fluorescence from that of the spinal cord image and expressed in arbitrary units.

The number of HRP-labeled axons were obtained from vibratome sections (Luo et al., 2002; Shi and Borgens, 2000; Shi and Pryor, 2000; Shi et al., 2001, 2002). The images were captured to a Macintosh Quadra 800 computer using a Leitz Ortoplan microscope and JVC video camera. The

numbers of HRP-labeled axons were counted and the final data were normalized per unit area and expressed as a density (axons/mm²).

Lactate dehydrogenase is usually confined inside the cell since it is unable to pass through the intact membrane. Therefore, the leakage of this enzyme to the extracellular space is indicative of membrane disruption (Koh and Choi, 1987). To detect LDH release, the solution bathing the cords was collected at the end of each treatment. The cord strips were quickly homogenized and the residual tissue LDH was assessed. LDH activity was immediately assayed using a lactate dehydrogenase test kit from Sigma (St. Louis, MO). The percentage of LDH release into the incubation solution was normalized to the total tissue LDH (sum of all the LDH leaked out of the tissue into the solution and supernatant collected) (Luo et al., 2002).

2.4. Measurement of oxidative stress

The extent of oxidative stress induced by acrolein in the spinal cord tissue was assessed by ROS generation, lipid peroxidation and protein carbonyl formation. Superoxide production was measured using hydroethidine (HE), which signifies the intracellular level of superoxide, as described in our previous paper (Luo et al., 2002). The fluorescence intensity of ethidium, formed after the oxidation of HE by ROS, was quantified and used as an index of superoxide levels.

Lipid peroxidation was analyzed using a lipid hydroperoxide assay kit from Cayman Chemical Company (Ann Arbor, MI), with 13-hydroperoxy octadecadienoic acid (13-HpODE) as the standard (Luo et al., 2002). Tissue lipid peroxide was expressed as nanomoles per 100 mg of wet tissue (nmol/100 mg).

Protein carbonyl in the crude homogenate was estimated according to Levine et al. (1990). Briefly, the sample (1 mg) was incubated with 0.5 ml of 10 mM 2,4-dinitrophenylhydrazine (DNPH) in 2N HCl (or 2N HCl alone for the blanks). The protein hydrazone derivatives were precipitated with 20% trichloroacetic acid, and the precipitates were washed with ethanol:ethyl acetate (1:1). The final pellet was resuspended and incubated in 6 M guanidine-HCl for 15 min at 37 °C. The carbonyl content was determined spectrophotometrically at 360 nm on the basis of molar absorbance coefficient of 22,000 M⁻¹ cm⁻¹.

2.5. Isolation of synaptosome and MTT test

After acrolein treatment, spinal cord segments were processed immediately to isolate synaptosomes according to a standard procedure (Keller et al., 1997). The synaptosomes were suspended in Locke's buffer (154 mM NaCl, 5.6 mM KCl, 2.3 mM CaCl₂, 1.0 mM MgCl₂, 3.6 mM NaHCO₃, 5 mM glucose, 5 mM HEPES) and were processed for an ³-[4,5-dimethylthiazol-2-yl]-2,5-diphenyltetrazolium bromide (MTT) test. Protein content was determined by bicinchoninic acid (BCA) protein assay kit from Pierce

Biotechnology Inc. (Rockford, IL), with bovine serum albumin as the standard.

The MTT tests performed in the present study were similar to those described by Keller et al. (1997). Briefly, a mixture of MTT (5 mg/ml) and succinate (15 mM) was added to a synaptosome suspension (MTT:synaptosome (1:10, v/v)) and allowed to incubate for 1 h at room temperature. Samples were then pelleted by centrifugation. The pellet was solubilized by 20% sodium dodecyl sulfate (pH 4.7). Absorbance of each sample was taken in triplicate with a plate reader (ATTC model 340, SLT Laboratory Instruments, Hillsborough, NC) at 550 nm. Results were expressed as a percent of the mean control value.

2.6. Chemicals

Lactate dehydrogenase kit, HRP, diaminobenzidine (DAB), sodium formate, PEG-catalase, and GEE were purchased from Sigma. Ethidium bromide, and HE were obtained from Molecular Probes (Eugene, OR). Mn(III)-tetrakis(*N*-methyl-4'-pyridyl) porphyrin and lipid peroxide assay kit were purchased from Cayman Chemical Company.

2.7. Statistic analysis

The data is expressed as a mean ± standard deviation (S.D.). The data was analyzed by one-way ANOVA using the statistics software package SPSS (version 11). Results showing overall significance were subjected to post-hoc least-significance difference test; *P* < 0.05 was considered statistically significant.

3. Results

3.1. Acrolein induces plasma membrane damage

The membrane damage induced by various concentrations of acrolein were assessed using three molecules with different molecular weights: EB (MW = 400 Da), HRP (MW = 44 kDa), and LDH (MW = 140 kDa).

3.1.1. EB uptake

After 4 h of exposure to acrolein (at concentrations of 1, 10, 25, 50, 100, and 200 μM), the plasma membrane permeability to EB was significantly increased in the spinal cord strips (*P* < 0.01 at all concentrations compared to control, *n* = 5) (Fig. 1A–C, F, and G). Time dependence of acrolein-mediated membrane damage was examined using acrolein at 10 and 200 μM (Fig. 1H). The durations of exposure were 15 min, 1, 2, and 4 h. At 200 μM of acrolein, the EB fluorescence of the cords exposed to acrolein for 15 min was 289 ± 23% of control, which is a significant increase (*P* < 0.005, *n* = 5). The EB uptake increased further during longer incubations of 1–4 h. Specifically, the

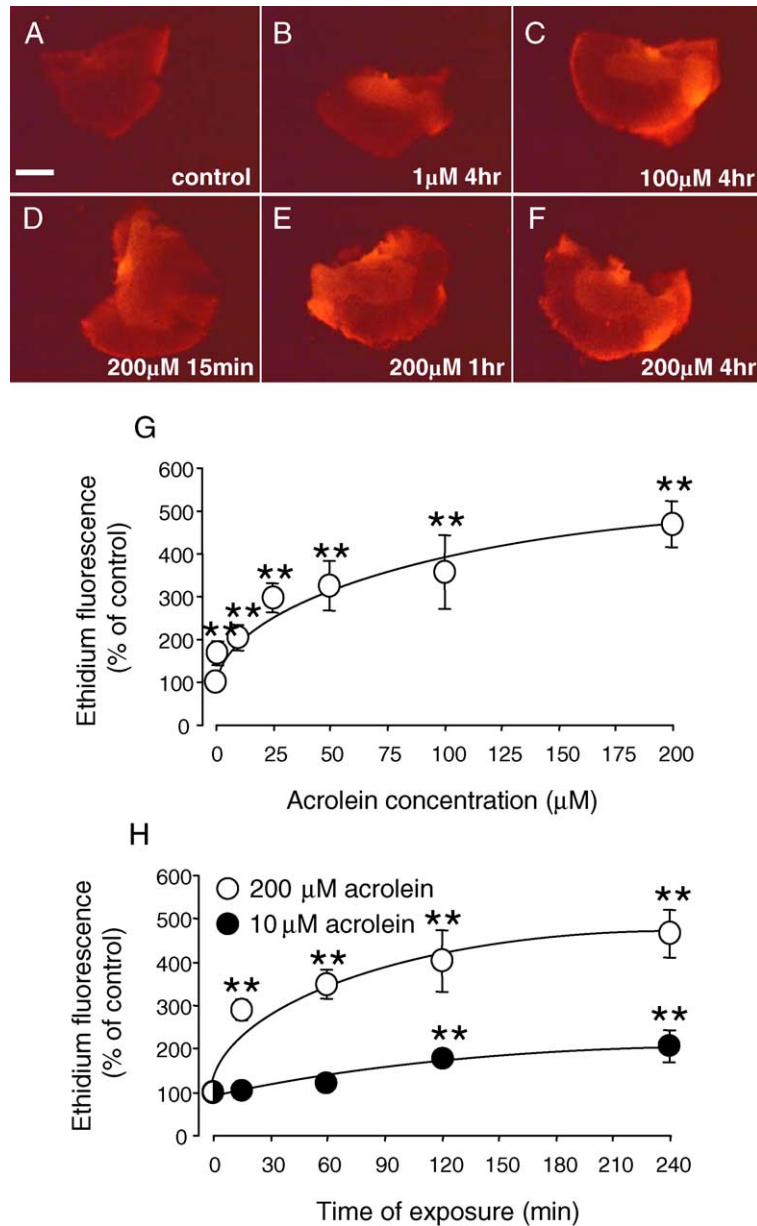


Fig. 1. Ethidium bromide fluorescence intensity in the spinal cord tissue exposed to different concentrations of acrolein at different time points. (A) Fluorescence intensity of a representative cross-section in the control group (non-acrolein exposure). (B and C) Representative images showing the ethidium bromide fluorescence intensity in the cords exposed to 1 μM (B) and 100 μM (C) acrolein for 4 h. Note the difference of EB fluorescence intensity between 1 and 100 μM . (D–F) Fluorescence intensity in the 200 μM group at 15 min (D), 60 min (E) and 4 h (F) following exposure. (G) Quantification of EB fluorescence intensity examined at 4 h post-injury as a function of acrolein concentration. The fluorescence intensity of the sample area was calculated using Sigmascan Pro and normalized by background subtraction (see Section 2). Fluorescence intensity is expressed as a percentage of the control group. Note the concentration-dependent increase of EB fluorescence intensity ($n = 5$). All the concentrations of acrolein tested (1–200 μM) significantly increased EB uptake. (H) Time course of EB fluorescence intensity in the spinal cords after exposure to 10 and 200 μM of acrolein. Half-filled circle indicates the overlap of the data from the group of 10 or 200 μM at the same time point. Note that acrolein exposure caused a concentration- and time-dependent increase of EB uptake. At 200 μM , all values post-injury were significantly different compared to pre-injury measurements. At 10 μM , however, only the values at 2 and 4 h post-injury were different from pre-injury measurements. In addition, the increase of EB permeability is significantly higher in 200 μM than 10 μM of acrolein at 1, 2, and 4 h post-injury. ** $P < 0.01$ with respect to control. Scale bar = 200 μm for (A–F).

EB uptake was 349 ± 34 , 401 ± 71 , and $467 \pm 55\%$ of control when exposed to acrolein for 1, 2, and 4 h ($P < 0.001$, $P < 0.0005$, and $P < 0.001$, respectively, $n = 5$ for all three groups) (Fig. 1). At 10 μM , the increase of EB uptake upon acrolein incubation was much less dramatic, which was

only significant after 1 and 2 h of exposure ($175.4 \pm 18.0\%$, $P < 0.01$, and $198.4 \pm 35.6\%$, $P < 0.0001$, respectively, when compared with control). Additionally, the increase of EB permeability was significantly higher in 200 μM than 10 μM acrolein at 1, 2, and 4 h post-injury ($P < 0.005$).

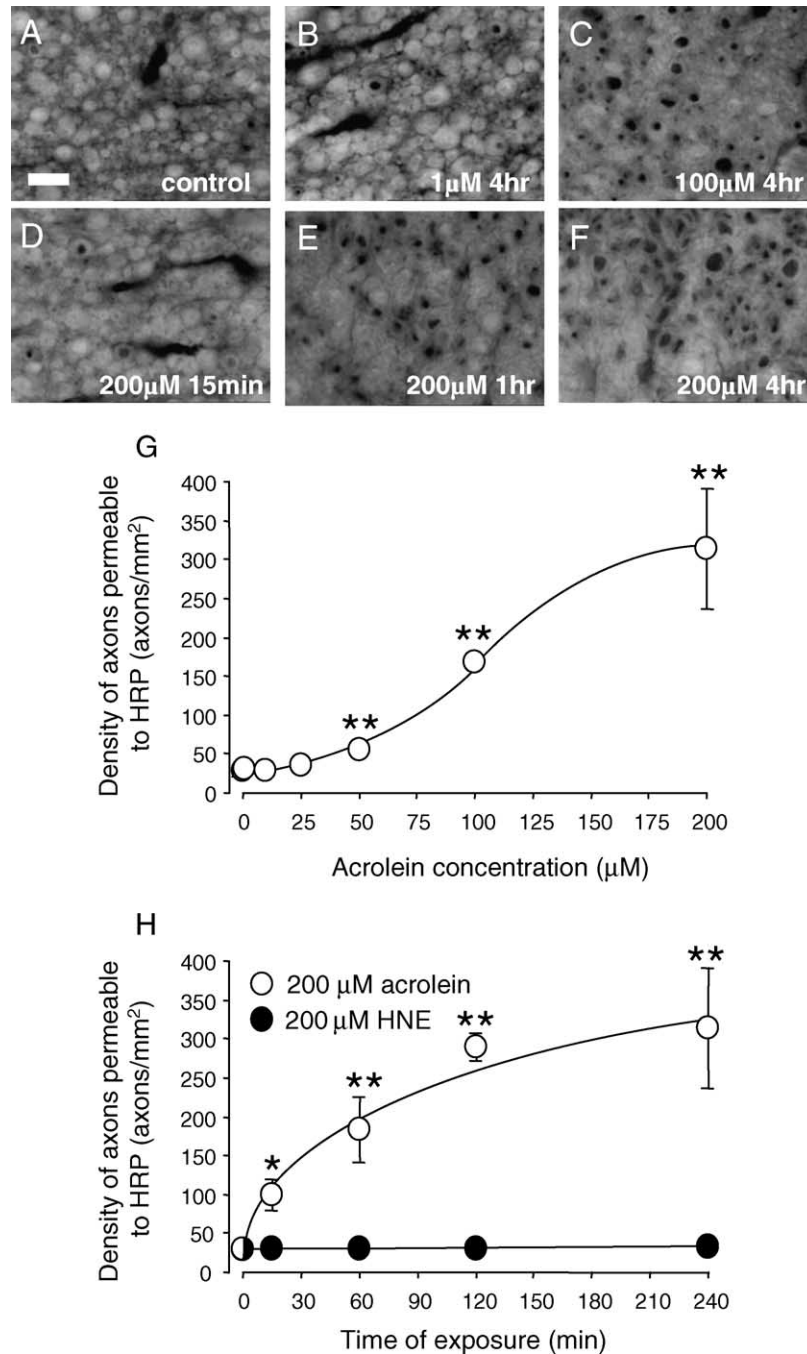


Fig. 2. Horseradish peroxidase uptake following acrolein exposure. (A) HRP labeling of a representative cross-section of spinal cord in the control group. Note the lack of axonal labeling. (B and C) Representative images showing HRP uptake in the cords exposed to 1 μM (B) and 100 μM (C) acrolein for 4 h. Note the difference of the density of HRP labeling between 1 and 100 μM . (D–F) HRP uptake in the 200 μM group at 15 min (D), 60 min (E) and 4 h (F) following exposure. Note the gradual increase of the numbers of HRP-labeled axons as the exposure time increases. (G) Quantification of HRP uptake as a function of acrolein concentration. The numbers of HRP-labeled axons were calculated and expressed as a density (axons/ mm^2) (see Section 2). Note the concentration-dependent increase of HRP uptake ($n = 5$). However, only higher concentrations of acrolein ($\geq 50 \mu\text{M}$) significantly increased HRP uptake ($n = 4–8$). (H) Time course of HRP uptake in the spinal cords after exposure to 200 μM of acrolein and HNE. In the acrolein-treated group, all values post-injury were significantly different compared to pre-injury measurements. Half-filled circle indicates the overlap of the data from the group using acrolein or HNE at the same time point. Note in the HNE treated group, HRP uptake was not significantly different from the control, in the time periods tested; while the same concentration of acrolein cause a time-dependent increase of HRP uptake. * $P < 0.05$, ** $P < 0.01$ with respect to control. Scale bar = 10 μm for (A–H).

3.1.2. HRP uptake

As shown in Fig. 2, plasma membranes became permeable to HRP in spinal cord strips exposed to 50, 100 and 200 μM acrolein for 4 h. Specifically, the numbers of axons showing HRP uptake were 54.33 ± 3.88 , 167 ± 7.57 , and 314 ± 77 axons/ mm^2 in strips exposed to 50, 100 and 200 μM acrolein. This was significantly higher than that of the control group ($P < 0.005$, $P < 0.0000005$, $P < 0.0000005$, respectively, $n = 5$ in all three groups). The HRP labeling in control was 29.4 ± 1.28 axons/ mm^2 (Fig. 1A and G). Significant HRP labeling was not found in cords exposed to acrolein at concentrations of 1, 10, and 25 μM for 4 h (31.3 ± 3.84 , 29.3 ± 2.03 , and 36.33 ± 4.67 axons/ mm^2 , respectively, $P > 0.05$ compared to control, $n = 5$ in all three groups).

In the experiments where cords were exposed to 200 μM acrolein at various times, significant HRP uptake was observed after 15 min, 1, 2, and 4 h of exposure. The numbers of axons labeled with HRP were 100 ± 20 axons/ mm^2 for 15 min exposure ($n = 5$), 184 ± 42 axons/ mm^2 for 1 h exposure ($n = 4$), 289 ± 18 axons/ mm^2 for 2 h exposure ($n = 8$), and 314 ± 77 axons/ mm^2 ($n = 7$) for 4 h of exposure to acrolein. All of these values are significantly higher than that measured in the controls ($P < 0.05$, $P < 0.005$, $P < 0.001$, and $P < 0.0000005$, respectively) (Fig. 2H).

We have also examined the time-dependent effect of HNE on membrane disruption at a concentration of 200 μM , similar to that used in studies of acrolein. It was clear that HNE at this concentration did not cause significant increase of HRP labeling during the 4 h period of exposure (Fig. 2H).

3.1.3. LDH release

Fig. 3A summarizes the experimental results evaluating the dose dependence of acrolein-mediated membrane damage, as revealed by the measurement of LDH in the extracellular space. The time of acrolein incubation was 4 h for all concentrations. The extracellular LDH in the control was $6.25 \pm 1.21\%$ of total (extracellular and intracellular). The concentration of LDH released to the extracellular space after 4 h of exposure to acrolein at 1, 10, 25, 50 and 100 μM was 6.28 ± 1.29 , 6.54 ± 1.30 , 6.95 ± 1.31 , 7.27 ± 1.57 , and $8.02 \pm 2.86\%$ of the total, respectively. None of these values was significantly different than that observed in control cords ($P > 0.05$, $n = 5$ for all four groups). However, significant increases in LDH release were measured in response to 200 μM acrolein ($13.98 \pm 3.02\%$, $P < 0.00005$ compared with control, $n = 5$).

The rate at which 200 μM induced LDH release was examined at various exposure times. As shown in Fig. 3B, LDH release increased gradually during the first 2 h, and dramatically during the subsequent 4 h period of observation. Specifically, LDH release was measured to be 6.15 ± 1.63 , 6.25 ± 1.25 , 7.85 ± 1.66 , and $13.98 \pm 3.02\%$, after 15 min, 1, 2 and 4 h exposure. Statistically significant elevation of LDH was only observed after 4 h exposure

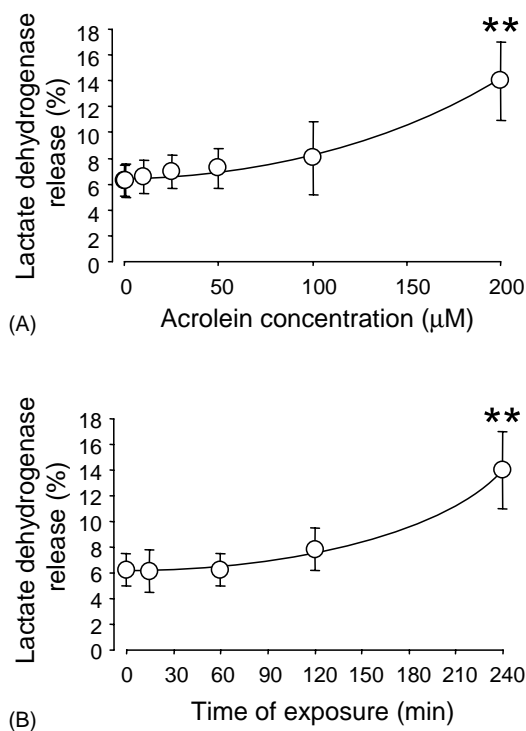


Fig. 3. LDH release after acrolein exposure. (A) LDH release measured after a 4 h exposure to acrolein of different concentrations. The solutions bathing the cords were collected at the end of exposure and assessed for LDH activity. Note as acrolein concentration increases, LDH release increases as well. However, only the concentration of 200 μM caused significant increase of LDH release ($n = 4$). (B) LDH release as a function of time in the 200 μM acrolein-treated group. The accumulation of LDH release at different time points after acrolein exposure (200 μM) was plotted. The LDH release increases as the exposure time increases. However, only after 4 h exposure did acrolein cause a significant increase of LDH release ($n = 5$). ** $P < 0.01$ with respect to control.

($P < 0.00005$, $n = 5$) but not at the shorter time periods ($P > 0.05$, $n = 5$ for all groups).

3.2. Acrolein induces oxidative stress

It has been reported that acrolein could induce ROS generation and exacerbate LPO (Adams Jr. and Klaidman, 1993; Patel, 1987). Therefore, we measured ROS and LPO levels in the spinal cord tissues following acrolein exposure. As shown in Fig. 4, superoxide generation (revealed by ethidium fluorescence) was increased in spinal cord strips exposed to 25, 50, 100, and 200 μM acrolein for 4 h (151.6 ± 11.2 , 171 ± 18 , 214 ± 20 , and $274 \pm 20\%$ of control, $P < 0.001$, $n = 6$ for all groups). There was no significant increase in superoxide in the strips exposed to 1, and 10 μM acrolein, however (104 ± 9 , and $115 \pm 17\%$ of control, $P < 0.05$, $n = 6$ for all groups) (Fig. 4G). In response to 200 μM acrolein, ethidium fluorescence increased steadily at 1, 2, and 4 h of exposure (234 ± 18 , 255 ± 26 , and $274 \pm 20\%$ of control, $P < 0.01$, $n = 6$) but not after 15 min of exposure ($141 \pm 11\%$ of control, $P > 0.05$, $n = 6$, Fig. 4H).

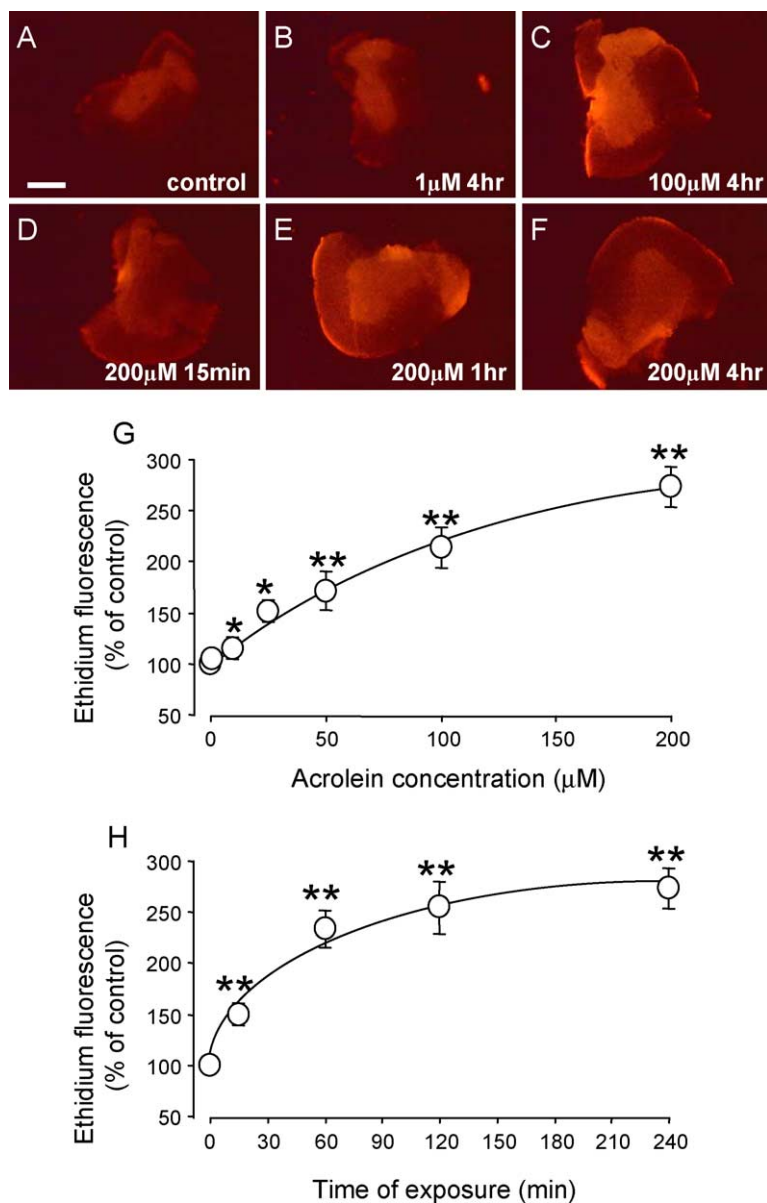


Fig. 4. ROS generation after acrolein exposure. ROS generation was detected using HE. Hydroethidine is oxidized to ethidium by ROS (superoxide), the fluorescence intensity of ethidium reflects ROS generation pro rata. (A) Fluorescence intensity of a representative cross-section in the control group (non-acrolein exposure). (B and C) Representative images showing the ethidium fluorescence intensity in the cords exposed to 1 μM (B) and 100 μM (C) acrolein for 4 h. Note the difference of ethidium fluorescence intensity between 1 and 100 μM . (D–F) Ethidium fluorescence intensity in the 200 μM group at 15 min (D), 1 h (E) and 4 h (F) following exposure. (G) Quantification of ethidium fluorescence intensity as a function of acrolein concentration. The fluorescence intensity of the sample area was calculated using Sigmascan Pro and normalized by background subtraction (see Section 2). Fluorescence intensity is expressed as a percentage of the control group. Note the concentration-dependent increase of EB fluorescence intensity ($n = 6$). The concentrations of acrolein at 25 μM or higher significantly increased EB uptake. (H) Examples of time course of EB fluorescence intensity in the spinal cords after exposure to 200 μM acrolein. Note that 200 μM acrolein caused significant increase of ROS generation at all of the time points tested (from 15 min to 4 h, $n = 6$). * $P < 0.05$, ** $P < 0.01$ with respect to control. Scale bar = 200 μm for (A–F).

The level of lipid peroxidation after acrolein exposure is shown in Fig. 5. Lipid peroxidation increased significantly in the spinal cord strips exposed to acrolein for 4 h at concentrations of 25 μM or higher. Specifically, the tissue LPO levels were 7.34 ± 1.58 , 8.53 ± 1.62 , 9.79 ± 2.22 and 12.74 ± 3.42 nmol/100 mg in strips exposed to 25, 50, 100 and 200 μM acrolein, respectively. All of these val-

ues are significantly higher than that of the control groups ($P < 0.05$ in all groups when compared to the controls, $n = 4$ for all groups). Similar measurement in control cords was only 4.86 ± 0.78 nmol/100 mg. The measurement of LPO in the strips exposed to 200 μM acrolein for various time periods showed that LPO increased significantly after 1 h exposure (12.74 ± 3.42 nmol/100 mg, $P < 0.01$,

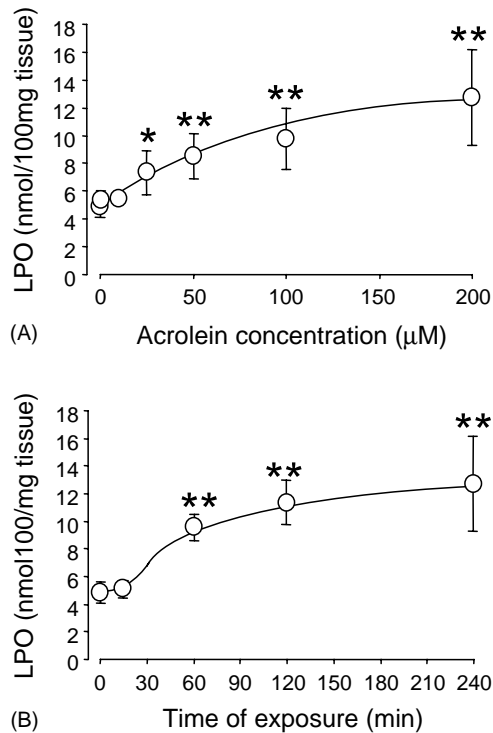


Fig. 5. Induction of lipid peroxidation after acrolein exposure. The extent of LPO was measured in homogenates of spinal cord segments after incubation in the absence of acrolein or in the presence of 1–200 μM acrolein. The evaluation of LPO was performed using a LPO assay kit. (A) LPO measured after a 4 h exposure of acrolein of different concentrations. Note as acrolein concentration increases, LPO release increases as well. However, only the concentrations of 25 μM or higher caused significant increase of LPO ($P < 0.01$, as compared with control, $n = 4$). (B) Lipid peroxidation as a function of time course in the 200 μM treated group. The LPO formation at different time points after acrolein exposure (200 μM) was plotted. The LPO increases as the exposure time increases, with significant increases at 1 h and thereafter (as compared with control, $n = 4$). * $P < 0.05$, ** $P < 0.01$ with respect to control.

$n = 4$), and continued to increase after 2 and 4 h of exposure (11.6 ± 0.79 , $P < 0.01$ and 9.50 ± 0.62 nmol/100 mg, $P < 0.001$, respectively, $n = 4$ for all groups).

Exposure of spinal cord tissue to increasing times of exposure and concentrations of acrolein promoted protein carbonyl formation in time- and concentration-dependent manners (Fig. 6). Note that 1 μM acrolein did not cause a significant increase of protein carbonyl formation during a 4 h period of exposure when compared to control ($P > 0.05$). However, 10 and 100 μM acrolein produced significant increase of protein carbonyl, at time periods ≥ 1 h. Specifically, 10 μM acrolein induced a significant increase at 1 h (4.77 ± 0.42 nmol/mg protein, $P < 0.05$, $n = 4$), 2 h (6.39 ± 0.27 nmol/mg protein, $P < 0.005$, $n = 4$), and 4 h (7.89 ± 0.41 nmol/mg protein, $P < 0.0001$, $n = 4$). At 100 μM , acrolein induced a significant increase of protein carbonyl at 15 min (4.05 ± 0.37 nmol/mg protein, $P < 0.05$, $n = 4$), 1 h (6.05 ± 0.33 nmol/mg protein, $P < 0.001$, $n = 4$), 2 h (9.31 ± 0.44 nmol/mg protein, $P < 0.001$, $n = 4$), and 4 h (14.8 ± 1.23 nmol/mg protein, $P < 0.0001$, $n = 4$).

In addition, a significant increase was detected in response to 100 μM acrolein than that detected in the 10 μM group at both 2 and 4 h post-injury ($P < 0.05$).

3.3. Treatment with antioxidants attenuates acrolein-induced membrane damage

Since oxidative stress is induced in the presence of acrolein, we reasoned that ROS could induce membrane disruption. Therefore, antioxidants should lessen acrolein-mediated membrane damage. As shown in Fig. 7, treatment with antioxidants reduced the acrolein-mediated membrane damage. After 2 h exposure to 200 μM acrolein, the density of HRP-labeled axons was 289 ± 18 axons/ mm^2 (Fig. 7). Treatment with glutathione, preincubation or simultaneous with acrolein exposure, PEG-catalase, sodium formate, and MnTMPyP added at the time of acrolein exposure, significantly decreased the density of HRP labeling (88 ± 10 , 99 ± 8 , 124 ± 8 , 141 ± 10 , and 157 ± 7 axons/ mm^2 , $P < 0.001$ compared to the untreated group, $n = 6$ for all the treatment groups). This demonstrates that ROS do contribute to acrolein-mediated membrane damage.

3.4. Acrolein inhibits mitochondrial function

In the next set of experiments, we examined the functional status of mitochondria in response to acrolein exposure since mitochondria are a rich source of ROS as well as a target of ROS attack. At 1 μM , acrolein did not cause significant mitochondrial functional impairment during a 4 h period of exposure ($P > 0.05$, $n = 5$ for all time points). However, at 10 μM , acrolein significantly decreased mitochondrial electron transport function, which was observed after 1 h ($88.5 \pm 5.4\%$ of control, $P < 0.01$), 2 h ($80.1 \pm 7.0\%$ of control, $P < 0.001$) and 4 h ($75.3 \pm 4.5\%$ of control, $P < 0.0001$) of exposure. The mitochondria functional decrease is more prominent for 100 μM acrolein than that of 10 μM acrolein at 1, 2, and 4 h of exposure ($P < 0.0001$, Fig. 8). Our results revealed that acrolein impairs the function of synaptosomal mitochondria, extracted from the acrolein-exposed cords, in a time- and concentration-dependent manner.

4. Discussion

4.1. Characteristics of acrolein-mediated membrane damage

In this study we report that acrolein, a product of membrane lipid peroxidation, inflicts severe plasma membrane damage in isolated guinea pig spinal cord in both a dose- and time-dependent manner. Since membrane damage is critical in triggering cellular deterioration leading to cell death (Fitzpatrick et al., 1998; Shi and Blight, 1996; Shi and Pryor, 2002), acrolein could contribute to functional loss

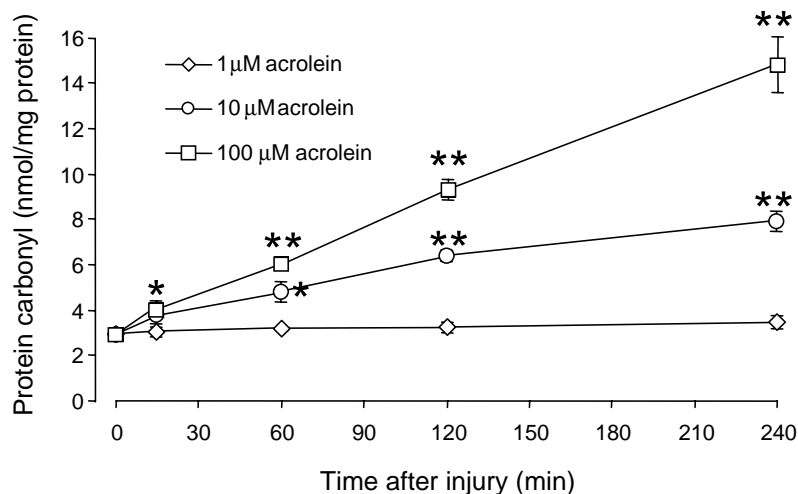


Fig. 6. Protein carbonyl formation after exposure of different concentrations of acrolein. Exposure of spinal cord tissue to increasing concentrations of acrolein promotes protein carbonyl formation in a time- and concentration-dependent manner. Spinal cord segments were exposed to different concentrations of acrolein and samples were collected at different time points after exposure. Levels of protein carbonyl were then quantified. Note 1 μM acrolein did not cause significant increase of protein carbonyl formation during a 4 h period of exposure, as compared with the control. In the 10 and 100 μM acrolein-treated groups, significantly increased protein carbonyl was observed after 1 h of exposure and thereafter ($n = 4$), with more pronounced increases in 100 μM than that in 10 μM group at 2 and 4 h post-injury. * $P < 0.05$, ** $P < 0.01$ with respect to control.

in neural disease and injury where ROS have been implicated. There are several characteristics of acrolein-mediated membrane damage worth pointing out. First, plasma membrane disruption induced by acrolein is a progressive process with a delay in the first evidence of damage ranging from minutes to hours. Conversely, the most severe plasma membrane leakage occurs immediately after physical trauma (Luo et al., 2002; Shi and Pryor, 2000; Shi et al., 2001). Membrane breaches gradually seal in a time-dependent man-

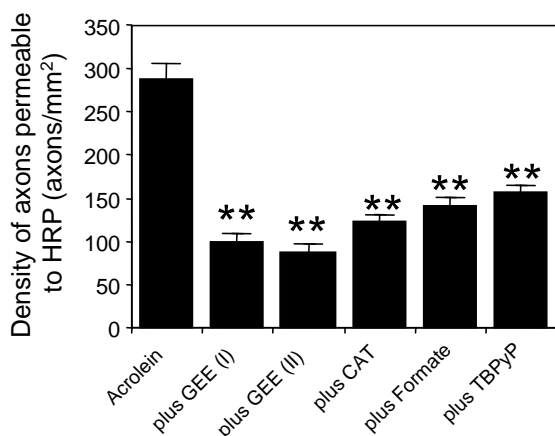


Fig. 7. Effects of the treatment with antioxidants on acrolein-induced HRP uptake. The antioxidants glutathione (GEE II, 2 mM), PEG-catalase (CAT, 500 U/ml), sodium formate (Formate, 15 mM), and MnTMPyP (25 μM) were added to the acrolein solution the spinal cord segments were bathed in. In a glutathione-pretreated group (GEE I), the spinal cord segments were immersed in glutathione solution for 2 h before being transferred to the acrolein solution. After a 4 h exposure, the number of HRP-labeled axons was quantified as described in Section 2. ** $P < 0.01$ with respect to untreated.

ner post-impact, revealed by a continued reduction of permeability to different molecular markers (Luo et al., 2002; Shi and Pryor, 2000; Shi et al., 2001). The delayed time course of acrolein-mediated membrane damage suggests that acrolein may play an important role in secondary, rather than primary, injury following mechanical trauma. Furthermore, our data also indicates that membrane breakdown cannot only be the result of physical insult, but also result from the exposure to chemical toxins over time.

The finding that acrolein at micromolar levels can induce significant membrane damage to healthy-uninjured tissue is very interesting. This indicates that acrolein is capable of inflicting delayed membrane damage to the nearby uninjured nerve tissue outside of the original compression site, should acrolein be stable enough and the environment permits an effective diffusion. The half-life of acrolein is estimated to be in the order of several hours, which is 100 billion times longer than that of the much-studied ROS (Esterbauer et al., 1991). Therefore, it is likely that acrolein is capable of diffusing to neighboring, otherwise healthy, tissue. Hence, we hypothesize that acrolein may act as a messenger toxin to inflict secondary and diffusive membrane damage following physical trauma. Consistent with this hypothesis, we have recently detected a significant elevation of acrolein and, more importantly, concomitant membrane damage, at more than 10 mm beyond the original impact site in a guinea pig spinal cord compression injury model (Luo et al., 2003).

To further support a possible role of acrolein in spinal cord injury, we have shown that acrolein is significantly more toxic than HNE, which has already been implicated in spinal cord injury (Baldwin et al., 1998; Springer et al., 1997). Specifically, at a concentration of 200 μM , HNE did

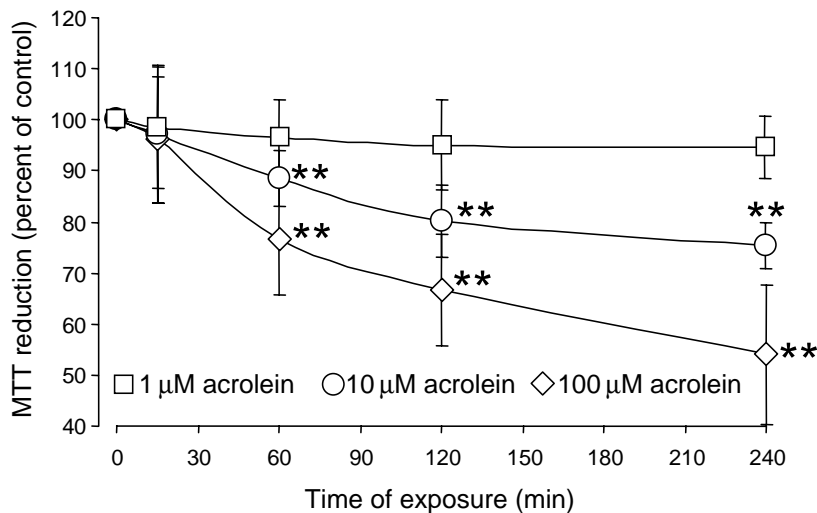


Fig. 8. Time course of mitochondrial function change (MTT test) after exposure of different concentrations of acrolein. At the end of each treatment, the synaptosome was isolated from the spinal cord and subjected to MTT test (see Section 2). The levels of MTT reduction were quantified and expressed as a percentage of control. Results were pooled from four independent experiments. Note 1 μM acrolein did not cause significant mitochondrial functional impairment during a 4 h period of exposure; with 10 and 100 μM acrolein, significantly decreased mitochondrial electron transport function was observed after 1 h exposure and thereafter. More significant decreases were observed in 100 μM group than that in 10 μM group at 1, 2, and 4 h. ** $P < 0.01$ with respect to control.

not cause significant HRP labeling when applied for 4 h, while acrolein at the same concentration inflicted significant membrane disruption beginning at 15 min of exposure (Fig. 2). This is consistent with the notion that acrolein is 100 times more reactive than HNE and may play a more significant role in various conditions (Esterbauer et al., 1991). In summary, we hypothesize that, as a potential key factor in inflicting prolonged and diffusive membrane disruption, acrolein may play a major role in cell death, tissue reduction and functional loss seen in both acute trauma and chronic CNS disorder.

4.2. Relevance of acrolein concentration in the current study

We have found that acrolein at a concentration as low as 1 μM can induce significant EB uptake after the cord was incubated with acrolein for 4 h (Fig. 1), while higher concentrations of acrolein would induce even more severe membrane damage. Acrolein at concentrations at 50 μM or higher caused significant HRP uptake. Our previous studies demonstrated that such membrane damage (detectable by HRP) could lead to compound action potential conduction as well as membrane potential loss (Shi and Borgens, 2000; Shi and Pryor, 2000; Shi et al., 2001, 2002).

We believe the concentrations of acrolein used in the current study are achievable in vivo. The level of acrolein in the sera of a normal human was measured to reach 50 μM (Satoh et al., 1999), and acrolein was measured to reach 80 μM in respiratory tract lining fluids as a result of smoking (Nardini et al., 2002). Furthermore, the toxicity of acrolein in in vivo injuries may be more severe than our

estimates due to two factors. First, the longest duration of acrolein incubation used in the current study was 4 h. In reality, however, acrolein may present for much longer times. We believe this is possible due to prolonged elevation of ROS and lipid peroxidation in various disorders (Baldwin et al., 1998; Hall, 1989; Springer et al., 1997). Therefore, as a byproduct of lipid peroxidation, the level of acrolein is also likely to initially be high and remain higher for extended periods. A second critical factor to consider is the half-life of acrolein (about several hours) (Esterbauer et al., 1991). Recently, we have obtained direct evidence that acrolein was increased 24 h following traumatic spinal cord injury. We used a unique protein binding method developed by Uchida and his colleagues (Satoh et al., 1999; Uchida et al., 1998), that allows detection of acrolein in tissues. We observed a significant increase in acrolein at 24 h following compression injury of guinea pig spinal cord (Luo et al., 2003). In addition to traumatic injury, the temporal increase of acrolein in chronic neurodegenerative disease such as Alzheimer's, is likely to be even longer (Lovell et al., 2001). Considering the time dependence of acrolein toxicity, it is reasonable to assume that the concentration threshold of acrolein toxicity in in vivo trauma is lower than 1 μM .

Ischemia can also exacerbate acrolein toxicity while it is damaging membranes (Peasley and Shi, in press). The mechanism of such exacerbation may be related to the increased generation of ROS, decreased production of ATP, and toxic accumulation of intracellular calcium as a result of ischemia (Lewen et al., 2000; Povlishock and Kontos, 1992). Since ischemia usually accompanies traumatic brain and spinal cord injury, the detrimental effect of acrolein in in vivo injury is

likely to be more severe than that determined in the current study where there was no shortage of oxygen.

4.3. The possible mechanisms of acrolein-mediated membrane disruption—the role of ROS

The mechanism of the action of acrolein-mediated membrane damage is not fully understood. However, two lines of experimental findings suggest that ROS may take part in this process. First, there is a significant increase of ROS, LPO, and protein carbonyl levels in response to acrolein exposure (Figs. 4–6). Second, acrolein-mediated membrane damage can be significantly reduced by the application of antioxidants. Therefore, it is likely that acrolein-induced membrane disruption is, at least in part, mediated by ROS.

It is interesting to point out that, out of all the antioxidants used, GEE, which can be easily converted to glutathione following entry to the cell, is the most effective in countering acrolein-mediated membrane damage (Fig. 7). This is likely due to: (1) the ability of glutathione to specifically detoxify acrolein by direct binding; and (2) its ability as a scavenger of H₂O₂ (Kehrer and Biswal, 2000). Other antioxidants, catalase, formate, and MnTMPyP, can significantly decrease the acrolein-mediated damage by at least 50% (Fig. 7). This further suggests that at least half of the acrolein-induced membrane damage is mediated by ROS. The rest of the detrimental effects of acrolein could be mediated by other intermediate compounds or acrolein itself.

The mechanism by which acrolein induces ROS generation and LPO in tissues is still an open issue. It is possible that several mechanisms are involved. First, acrolein can be directly transformed to superoxide by xanthine oxidase or aldehyde dehydrogenase—both are known to exist in nervous tissue (Adams Jr. and Klaidman, 1993). Second, acrolein causes ROS elevation by depleting endogenous antioxidants, such as glutathione (Kehrer and Biswal, 2000). Third, other mechanisms, such the activation of phospholipase A₂ (Fukuda et al., 1999), the elevation of intracellular calcium (Lovell et al., 2000), and the accumulation of iron (Ciccoli et al., 1994) may also play roles in ROS production as a result of acrolein exposure.

Giving their central role in oxidative metabolism, mitochondria may also play a significant role in ROS accumulation. This is because mitochondria are a rich source of ROS, as well as a primary site of energy production. It is well established that mitochondrial dysfunction will not only hinder the effectiveness of the endogenous antioxidant system, but also encourage the elevation and release of ROS from mitochondria. Furthermore, mitochondrial dysfunction also causes more calcium release from mitochondria (a calcium reservoir)—causing more “positive feedback” mechanism and cytosol damage. We report here that mitochondrial function is indeed significantly hampered in response to acrolein attack (Fig. 8); such mitochondrial dysfunction would further increase oxidative stress.

4.4. Significance of current findings in other disorders

Acrolein is a ubiquitous pollutant in the environment (Levaggi and Feldstein, 1970), a major unsaturated aldehyde in gas-phase cigarette smoking (Triebig and Zober, 1984), and a major metabolite of cyclophosphamide (Patel, 1990), an anticancer drug. Therefore, acrolein-induced membrane damage may be an important pathogenic mechanism leading to cell death and functional loss in a variety of medical conditions. Understanding the characteristics and the mechanism of acrolein-mediated membrane damage is likely to be beneficial not only to unveil the pathology underlying these disorders, but as well to suggest effective therapeutic interventions.

Acknowledgements

This study was supported by grant NS-33687 from NIH-NINDS, funding from both Purdue University and the State of Indiana. We thank Dr. Richard Borgens for his support and encouragement. We also thank Phyllis Zickmund, Nianyu Li and Dr. J. Paul Robinson for their invaluable assistance.

References

- Adams Jr., J.D., Klaidman, L.K., 1993. Acrolein-induced oxygen radical formation. *Free Radic. Biol. Med.* 15, 187–193.
- Baldwin, S.A., Broderick, R., Osbourne, D., Waeg, G., Blades, D.A., Scheff, S.W., 1998. The presence of 4-hydroxynonenal/protein complex as an indicator of oxidative stress after experimental spinal cord contusion in a rat model. *J. Neurosurg.* 88, 874–883.
- Ciccoli, L., Signorini, C., Alessandrini, C., Ferrali, M., Comporti, M., 1994. Iron release, lipid peroxidation, and morphological alterations of erythrocytes exposed to acrolein and phenylhydrazine. *Exp. Mol. Pathol.* 60, 108–118.
- Coyle, J.T., Puttfarcken, P., 1993. Oxidative stress, glutamate, and neurodegenerative disorders. *Science* 262, 689–695.
- Dennis, K.J., Shibamoto, T., 1990. Gas chromatographic analysis of reactive carbonyl compounds formed from lipids upon UV-irradiation. *Lipids* 25, 460–464.
- Droge, W., 2002. Free radicals in the physiological control of cell function. *Physiol. Rev.* 82, 47–95.
- Esterbauer, H., Schaur, R.J., Zollner, H., 1991. Chemistry and biochemistry of 4-hydroxynonenal, malonaldehyde and related aldehydes. *Free Radic. Biol. Med.* 11, 81–128.
- Farooqui, A.A., Horrocks, L.A., 1998. Lipid peroxides in the free radical pathophysiology of brain diseases. *Cell. Mol. Neurobiol.* 18, 599–608.
- Fitzpatrick, M.O., Maxwell, W.L., Graham, D.I., 1998. The role of the axolemma in the initiation of traumatically induced axonal injury. *J. Neurol. Neurosurg. Psychiatry* 64, 285–287 (Editorial).
- Fukuda, T., Kim, D.K., Chin, M.R., Hales, C.A., Bonventre, J.V., 1999. Increased group IV cytosolic phospholipase A₂ activity in lungs of sheep after smoke inhalation injury. *Am. J. Physiol.* 277, L533–L542.
- Hall, E.D., 1989. Free radicals and CNS injury. *Crit. Care Clin.* 5, 793–805.
- Hall, E.D., 1996. Lipid peroxidation. *Adv. Neurol.* 71, 247–257 (Discussion, pp. 257–248).

- Kehrer, J.P., Biswal, S.S., 2000. The molecular effects of acrolein. *Toxicol. Sci.* 57, 6–15.
- Keller, J.N., Mark, R.J., Bruce, A.J., Blanc, E., Rostein, J.D., Uchida, K., Waeg, G., Mattson, M.P., 1997. 4-Hydroxynonenal, an aldehydic product of membrane lipid peroxidation, impairs glutamate transport and mitochondrial function in synaptosomes. *Neuroscience* 80, 685–696.
- Koh, J.Y., Choi, D.W., 1987. Quantitative determination of glutamate mediated cortical neuronal injury in cell culture by lactate dehydrogenase efflux assay. *J. Neurosci. Methods* 20, 83–90.
- Krause, T.L., Fishman, H.M., Ballinger, M.L., Bittner, G.D., 1994. Extent and mechanism of sealing in transected giant axons of squid and earthworms. *J. Neurosci.* 14, 6638–6651.
- Lenaz, G., 2001. The mitochondrial production of reactive oxygen species: mechanisms and implications in human pathology. *IUBMB Life* 52, 159–164.
- Levaggi, D.A., Feldstein, M., 1970. The determination of formaldehyde, acrolein, and low molecular weight aldehydes in industrial emissions on a single collection sample. *J. Air Pollut. Control Assoc.* 20, 312–313.
- Levine, R.L., Garland, D., Oliver, C.N., Amici, A., Climent, I., Lenz, A.G., Ahn, B.W., Shaltiel, S., Stadtman, E.R., 1990. Determination of carbonyl content in oxidatively modified proteins. *Methods Enzymol.* 186, 464–478.
- Lewen, A., Matz, P., Chan, P.H., 2000. Free radical pathways in CNS injury. *J. Neurotrauma* 17, 871–890.
- Lovell, M.A., Xie, C., Markesbery, W.R., 2000. Acrolein, a product of lipid peroxidation, inhibits glucose and glutamate uptake in primary neuronal cultures. *Free Radic. Biol. Med.* 29, 714–720.
- Lovell, M.A., Xie, C., Markesbery, W.R., 2001. Acrolein is increased in Alzheimer's disease brain and is toxic to primary hippocampal cultures. *Neurobiol. Aging* 22, 187–194.
- Luo, J., Borgens, R.B., Shi, R., 2002. Polyethylene glycol immediately repairs neuronal membranes and inhibits free radical production after acute spinal cord injury. *J. Neurochem.* 83, 1–10.
- Luo, J., Uchida, K., Shi, R., 2003. Lipid peroxidation products, acrolein and 4-hydroxynonenal, are increased following traumatic spinal cord injury in guinea pig. 33rd Society for Neuroscience annual meeting neurobiology of lipids sessions. Published online Oct 1, 2003. Available at: <http://www.neurobiologyoflipids.org/content/2/3>. *Neurobiol. Lipids* 2 (3).
- Meiri, H., Spira, M.E., Parnas, I., 1981. Membrane conductance and action potential of a regenerating axon tip. *Science* 211, 709–712.
- Nardini, M., Finkelstein, E.I., Reddy, S., Valacchi, G., Traber, M., Cross, C.E., Van der Vliet, A., 2002. Acrolein-induced cytotoxicity in cultured human bronchial epithelial cells. Modulation by alpha-tocopherol and ascorbic acid. *Toxicology* 170, 173–185.
- Patel, J.M., 1987. Stimulation of cyclophosphamide-induced pulmonary microsomal lipid peroxidation by oxygen. *Toxicology* 45, 79–91.
- Patel, J.M., 1990. Metabolism and pulmonary toxicity of cyclophosphamide. *Pharmacol. Ther.* 47, 137–146.
- Peasley, M., Shi, R. Ischemic insult exacerbates acrolein-induced conduction loss and axonal membrane disruption in guinea pig spinal cord white matter. *J. Neurologic. Sci.*, in press.
- Pettus, E.H., Christman, C.W., Giebel, M.L., Povlishock, J.T., 1994. Traumatically induced altered membrane permeability: its relationship to traumatically induced reactive axonal change. *J. Neurotrauma* 11, 507–522.
- Povlishock, J.T., Kontos, H.A., 1992. The role of oxygen radicals in the pathobiology of traumatic brain injury. *Hum. Cell* 5, 345–353.
- Satoh, K., Yamada, S., Koike, Y., Igarashi, Y., Toyokuni, S., Kumano, T., Takahata, T., Hayakari, M., Tsuchida, S., Uchida, K., 1999. A 1-hour enzyme-linked immunosorbent assay for quantitation of acrolein- and hydroxynonenal-modified proteins by epitope-bound casein matrix method. *Anal. Biochem.* 270, 323–328.
- Shi, R., Blight, A.R., 1996. Compression injury of mammalian spinal cord in vitro and the dynamics of action potential conduction failure. *J. Neurophysiol.* 76, 1572–1580.
- Shi, R., Borgens, R.B., 2000. Anatomic repair of nerve membrane in crushed mammalian spinal cord with polyethylene glycol. *J. Neurocytol.* 29, 633–644.
- Shi, R., Pryor, J.D., 2000. Temperature dependence of membrane sealing following transection in mammalian spinal cord axons. *Neuroscience* 98, 157–166.
- Shi, R., Pryor, J.D., 2002. Pathological changes of isolated spinal cord axons in response to mechanical stretch. *Neuroscience* 110, 765–777.
- Shi, R., Asano, T., Vining, N.C., Blight, A.R., 2000. Control of membrane sealing in injured mammalian spinal cord axons. *J. Neurophysiol.* 84, 1763–1769.
- Shi, R., Qiao, X., Emerson, N., Malcom, A., 2001. Dimethylsulfoxide enhances CNS neuronal plasma membrane resealing after injury in low temperature or low calcium. *J. Neurocytol.* 30, 829–839.
- Shi, R., Luo, J., Peasley, M.A., 2002. Acrolein inflicts axonal membrane disruption and conduction loss in isolated guinea pig spinal cord. *Neuroscience* 115, 337–340.
- Springer, J.E., Azbill, R.D., Mark, R.J., Begley, J.G., Waeg, G., Mattson, M.P., 1997. 4-Hydroxynonenal, a lipid peroxidation product, rapidly accumulates following traumatic spinal cord injury and inhibits glutamate uptake. *J. Neurochem.* 68, 2469–2476.
- Triebig, G., Zober, M.A., 1984. Indoor air pollution by smoke constituents—a survey. *Prev. Med.* 13, 570–581.
- Uchida, K., 1999. Current status of acrolein as a lipid peroxidation product. *Trends Cardiovasc. Med.* 9, 109–113.
- Uchida, K., Kanematsu, M., Sakai, K., Matsuda, T., Hattori, N., Mizuno, Y., Suzuki, D., Miyata, T., Noguchi, N., Niki, E., Osawa, T., 1998. Protein-bound acrolein: potential markers for oxidative stress. *Proc. Natl. Acad. Sci. U.S.A.* 95, 4882–4887.
- Xie, X., Barrett, J.N., 1991. Membrane resealing in cultured rat septal neurons after neurite transection: evidence for enhancement by Ca²⁺-triggered protease activity and cytoskeletal disassembly. *J. Neurosci.* 11, 3257–3267.
- Yawo, H., Kuno, M., 1983. How a nerve fiber repairs its cut end: involvement of phospholipase A₂. *Science* 222, 1351–1352.